Mon. Not. R. astr. Soc. (1985) **217**, 787–804

A numerical study of the stability of spherical galaxies

David Merritt and Luis A. Aguilar *Department of Astronomy, University of California, Berkeley, CA 94720, USA*

Accepted 1985 July 10. Received 1985 July 8; in original form 1985 May 29

Summary. We examine the stability of spherical, non-rotating galaxies by using an N-body code to evolve a set of initially equilibrium models generated from three distribution functions. All models have the same initial density profile, essentially a de Vaucouleurs law. The first family is characterized by a velocity ellipsoid that becomes more radial outwards; the second is most radial at the centre; and the third has a constant anisotropy. All three families are unstable to the formation of a bar when the velocity distribution is sufficiently anisotropic. In the first family the transition to instability appears to occur suddenly as the anisotropy is increased, while the other two families appear to be unstable even for very small total anisotropies. Our results are inconsistent with a recent proof of the stability of a wide class of anisotropic systems.

The instability of radially anisotropic models suggests that an initially spherical cloud that is sufficiently cold will form a bar during its collapse. To test this hypothesis, we have simulated the collapse and virialization of galaxies starting from spherical initial conditions with various temperatures. We find that putting less than ~10 per cent of the initial energy in random motions leads to the formation of a bar. The instability appears to be very effective at erasing 'memory' of the initial conditions; in particular, it greatly reduces the dependence of the final central concentration on the initial temperature.

1 Introduction

The possibility that stellar dynamical models describing elliptical galaxies might be subject to global instabilities, in much the same way that models for disc galaxies are often found to be unstable, has been the subject of a growing number of studies. Because of the difficulty of constructing equilibrium triaxial models, all of this work has concentrated on the spherical case. Antonov (1960, 1962) showed more than two decades ago that any spherical, isotropic model, defined by a phase-space distribution function f that depends only on orbital energy E, is stable if $df/dE<0$ and $d^3\varrho/d\Phi^3\leq 0$; here $\varrho(r)$ and $\Phi(r)$ are the spatial density and gravitational potential, respectively. All the isotropic models that are commonly used to represent elliptical galaxies satisfy these criteria. On the other hand, Fridman & Polyachenko (1984, vols 1 and 2; hereafter FP1 and FP2) reproduce a proof, attributed to Antonov, that any model composed of purely *radial* orbits is *un*stable. The instability was apparently first verified by Polyachenko (1981) using an N-body code. He computed the evolution of a radial orbit model with initial density profile $\varrho \propto r^{-2}$, and showed that it evolves irreversibly into an elongated, triaxial bar. Polyachenko & Shukhman (1981; see also FP1) addressed the question of how radially anisotropic a model must be before it becomes unstable to the formation of a bar. They analysed three families of models with variable anisotropy, and predicted instability when twice the ratio of kinetic energies in radial to tangential motions, $2T_r/T_t$ (equal to one for isotropic models), exceeded an average value of ~ 1.7. One of these families [the Henon (1973) generalized polytropes] was analysed independently by Barnes, Goodman & Hut (1985, hereafter BGH) using an N-body code. They found instability for $2T_r/T_t \gtrsim 1.4$, quite close to the value (1.43) predicted by the Soviet workers for this family (FP1). BGH also found some instabilities associated with a preponderance of nearly circular orbits. These instabilities seem less interesting from a physical point of view and will not be considered here.

Although a general theory of the stability of anisotropic galaxies is still lacking, the bar-making instability found by the Soviet workers appears to be closely related to the classical Jeans instability of a cold self-gravitating medium (FP2; BGH). In this interpretation, a spherical galaxy is unstable when the stellar 'pressure' in the tangential direction is insufficient to suppress gravitational clumping of nearly radial orbits about an axis of symmetry. The growing ellipsoidal deformation increases the tangential velocities and eventually stabilizes the system, but not before permanently destroying the spherical symmetry. Bars formed in this way can apparently be quite elongated, at least 2:1 (i.e. E5), which is not far from the maximum elongation observed in real elliptical galaxies.

The work published so far on stability of anisotropic spherical galaxies leaves unanswered a number of astrophysically important questions. The purpose of the present paper is to address some of these questions, namely: (i) What are the stability properties of spherical models with realistic density profiles? Past work was based on polytropes and other, not-very-centrally-concentrated models. (ii) Is the instability strongly dependent on the form of the distribution function, or can it be predicted from a global 'anisotropy parameter', as Fridman & Polyachenko suggest? (iii) Could the instability play an *active* role in galaxy formation, e.g. by determining the equilibrium flattening of a galaxy that formed via near-radial collapse?

A complete theoretical description of the instability is likely to be very difficult, especially in its non-linear stages, so we have decided on a purely phenomenological approach using an N-body code.

2 Computational method

We used essentially the same N-body code described by Aguilar & White (1985). The potential is computed at each time step from a truncated expansion in spherical harmonics (*cf.* Aarseth 1967); in the present case, terms up to quadrupolar order were retained. The radial resolution is determined essentially by the softening length ε associated with each particle. Very small values of ε allow the potential to be represented well at all radii, but are computationally bad because of the discontinuities that arise whenever the radii of two particles interchange ('shell crossings'; *cf.* McGlynn 1984). Large values of ε give the best energy conservation but do not allow orbits passing near the centre to be accurately represented. This problem is especially acute in the present calculations because of the very radial nature of the velocity distribution, which requires a large fraction of the particles to pass very close to the centre. Furthermore, in any model dominated by radial orbits, the density must diverge at least as fast as $\sim r^{-2}$ near the centre (Richstone & Tremaine 1984), implying a force that diverges as $\sim r^{-1}$. This means that a small error in representing the central potential can have a large effect on the global dynamics. The relevant quantity here is the ratio of the softening length ε to the maximum orbital pericentre $p_{\max}$. Since all orbits pass below $p_{\max}$, an accurate representation of the potential generally requires $\varepsilon \ll p_{\max}$. The number of particles must also be sufficiently large that a significant fraction remain inside $p_{\max}$.

In practice, relaxation effects associated with small softening lengths are relatively mild, and the most serious disadvantage of using a very small value of ε is the necessity of decreasing the integration time-step (S. White, private communication). Nevertheless we decided to evolve our first family of models with three different values of ε to see which of the features of the instabilty are dependent on the softening length. Much of our uncertainty about the precise boundary between stable and unstable models will result from numerical problems associated with the softening.

The quantity of primary importance in judging whether a particular model is unstable to the formation of a bar is the degree of elongation. We estimated the elongation by computing the moment of inertia tensor in stages, starting with the most bound particles and working outwards in binding energy. The results will be expressed in terms of the axis ratios X/Z and X/Y (where $X>Y>Z$) of the uniform ellipsoids having the same ratios of eigenvalues. This procedure allows one to recognize flattening both in the inner and outer regions.

The code uses a fourth-order predictor–corrector algorithm to advance particle positions. Particles within roughly one half-mass radius are advanced with one-fourth the time-step of those farther out. Time-steps quoted below refer to the outer region. This feature of the code is particularly important when dealing with highly centrally concentrated initial conditions, or strong collapses.

All quantities will henceforth be given in units such that the total mass M, the initial half-mass radius r_0, and Newton's constant G are equal to one. These units may be scaled to values appropriate to real galaxies using the relations

$$M=10^{10} a M_{\odot}, \qquad r_0=b \text{ kpc},$$

$$[t]=5.67\times 10^6 (b^3/a)^{1/2} \text{ yr}, \qquad [v]=173\ (a/b)^{1/2} \text{ km s}^{-1},$$

with a and b arbitrary constants. The half-mass crossing time, defined as the ratio of the half-mass radius to the root mean square velocity in the models described below, is 2.45 in these units. Computational time was about 8 hr on a VAX 11/780 for a typical run with 5000 particles and 1000 time-steps.

3 Stability of a family of anisotropic models

3.1 Initial conditions

Since observed elliptical galaxies are remarkably uniform in their radial structure, an ideal set of initial conditions would consist of a family of spherical models with the same mass distribution, but different orbital compositions. We have assumed for the initial density law of our models the form

$$\varrho(r)=\frac{M}{4\pi r_0^3}\left(\frac{r}{r_0}\right)^{-2}\left(1+\frac{r}{r_0}\right)^{-2}, \tag{1}$$

where M is the total mass and r_0 the half-mass radius. Equation (1) was proposed by Jaffe (1983) as a good fit to the (deprojected) luminosity profiles of observed galaxies. It is essentially identical to a de Vaucouleurs density law for $0.1 \leqslant r/r_0 \leqslant 10$; at smaller radii, equation (1) rises more steeply.

A particular family of phase-space distribution functions that exactly reproduce the density law (1) was derived by Merritt (1985b). These are characterized by a single free parameter r_a, the

Table 1. Parameters of the three families of equilibrium models.

Family 1.	r_a	0	0.1	0.2	0.3	0.5	1000		
	$2T_r/T_t$	∞	4.4	2.9	2.3	1.8	1.0		
	p_{max}	0	0.19	0.33	0.46	0.71	1000		
	symbol	●	x	△	■	o	–		
Family 2.	α	1	0.53	0.38	0.30	0.21	0.12	0.063	0
	$2T_r/T_t$	∞	4.4	2.9	2.3	1.8	1.4	1.2	1.0
	symbol	●	x	△	■	o	▲	□	–
Family 3.	m	-1.0	-0.75	-0.71	-0.67	-0.60	-0.50	0.	
	$2T_r/T_t$	∞	4.0	3.5	3.0	2.5	2.0	1.0	
	symbol	●	x	△	■	o	▲	–	

'anisotropy radius', which determines the degree of velocity anisotropy through the relation

$$\frac{\sigma_r^2}{\sigma_t^2}=1+\frac{r^2}{r_a^2} \tag{2}$$

with σ_r and σ_t the (one-dimensional) velocity dispersions in the radial and tangential directions. The models are isotropic in the centre and radial for $r \gg r_a$, which makes them good approximations to the galaxies formed in radial collapse simulations (van Albada 1982). Setting r_a to 0 gives the purely radial orbit model, and $r_a \to \infty$ gives the isotropic model. An algorithm for generating initial positions and velocities from the distribution function was verified, for $r_a=0.1\,r_0$, by integrating the equations of motion of a set of 5000 particles in the *fixed* potential corresponding to the density (1). The particle distribution showed random fluctuations consistent with the finite number of particles but no secular evolution.

Our primary motivation for choosing the density law (1) is that it diverges as strongly as r^{-2} at small radii, and can therefore be constructed from a completely radial set of orbits. Density laws that diverge more slowly toward the centre (e.g. de Vaucouleurs) or have a finite central density (e.g. Michie–King) require some minimum amount of tangential motion if their phase-space density is to satisfy Jeans's theorem (Richstone & Tremaine 1984). Although we do not consider a radial orbit model to be a very probable representation of a real galaxy, the expected instability should manifest itself most strongly in this case.

3.2 CHARACTER OF THE INSTABILITY

We have computed the evolution of a set of six equilibrium models with $r_a=\{0, 0.1, 0.2, 0.3, 0.5, 1000\}$. The last model is essentially isotropic and guaranteed to be stable; it serves as a control. Table 1 lists the initial values of the anisotropy parameter $2T_r/T_t$ (equal to one for an isotropic model), and of the radius p_{max} of the greatest orbital pericentre, for all of the models. Each model was evolved with three different values for the softening length, $\varepsilon=\{0.003, 0.01, 0.03\}$. A time-step of 0.05 was found to conserve energy to <3 per cent over an evolution time of 50 in the runs with the two larger softenings; decreasing the time-step a factor of 2 made no appreciable change in the final state in these runs. The runs with $\varepsilon=0.003$ required a time-step of 0.025 for the same accuracy; to avoid excessive computational times, these runs were made with half the number of particles (2500) as in the other runs (5000).

Fig. 1 illustrates the evolution of the $r_a=0.1$ model, computed with the medium softening $\varepsilon=0.01$. The model is clearly unstable; by $t=5$ (roughly two half-mass crossing times) a definite

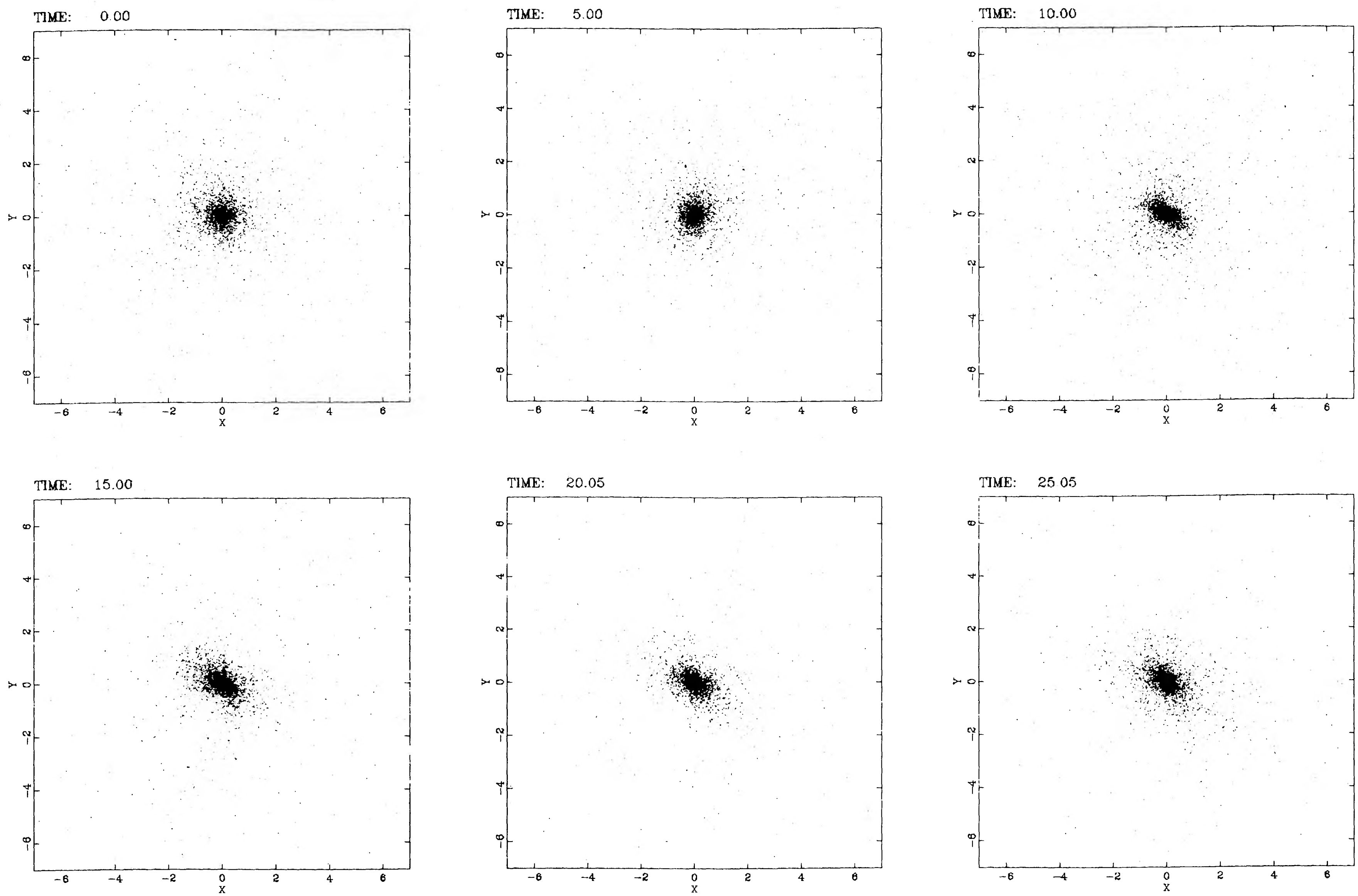

Figure 1. Snapshots of the run $\{r_a=0.1, \varepsilon=0.01\}$ at six time-steps. The view is from a direction such that the principle axes at the final time-step lie in the plane of the paper.

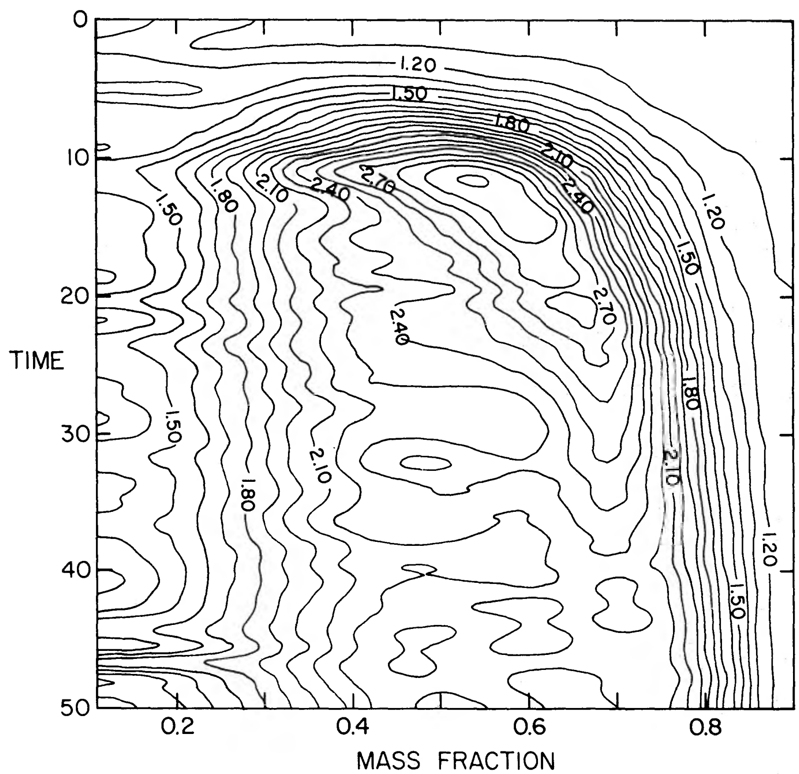

Figure 2. Evolution of the elongation of the model shown in Fig. 1. The contours are level surfaces of the axis ratio X/Z defined in the text.

deformation can be seen, and by $t\approx 10$ the elongation in the central regions has reached a maximum. The number of stars that share in the instability appears to increase monotonically with time; by $t=25$ all the mass within $r\approx 5$ appears to be elongated about a common axis. These subjective impressions can be verified in Fig. 2, which is a contour plot of the elongation as a function both of time, and of the fraction of particles considered, ranked according to their binding energy at each time-step. All of the model between the 20 and 85 per cent mass levels has attained an elongation of at least 3:2 by the final time-step; between the 40 and 80 per cent mass levels the axis ratio is nearly constant at ~ 2.2. The elongation of the bar reaches a temporary maximum of ~ 3 in the inner regions before relaxing to its final state. The position angles of the major axes of the bar (not shown in Fig. 2) vary by less than 20° between the 20 and 80 per cent mass levels at the final time-step. The bar is nearly prolate; the ratio of intermediate to short axes is ~ 1.2 for the inner 80 per cent of the mass. Although the final state is very close to axisymmetric, the major axes of the bar appear to wander somewhat during its early formation, and it is not clear that the instability can be described as a strictly axisymmetric one.

To test whether the evolution of the bar might be affected by the small number of terms (dipole and quadrupole) used by the computer code to approximate the non-spherical part of the potential, we repeated this run with a modified version of the code containing terms up to octupole order. The most bound 80 per cent of the mass reached maximum and final elongations of 2.7 and 2.1 respectively, compared to 2.9 and 2.3 with the quadrupolar code; there were no significant differences in the time dependence of the elongation. We conclude that our results are not likely to be strongly affected by the limited angular resolution of the code.

Comparison of the various runs allows us to make the following generalizations about the character of the instability in these models.

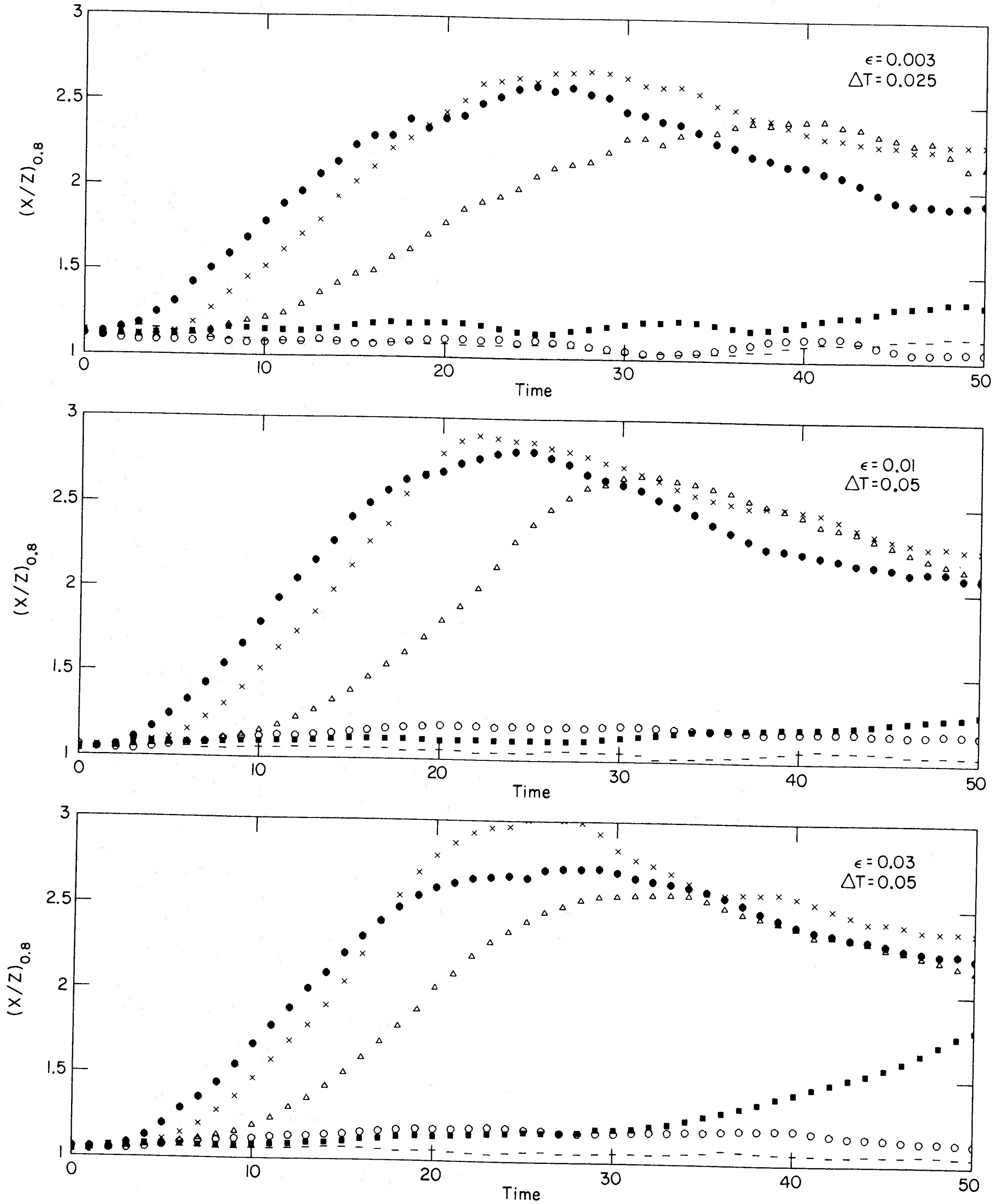

Figure 3. Evolution of the axis ratios of the most bound 80 per cent of the mass for each of the models from Family 1. Symbols are defined in Table 1.

(i) *The boundary between stable and unstable models is fairly sharp*. Fig. 3 shows the evolution of the axis ratios of the most bound 80 per cent of the mass for each of the runs. The models with $r_a=\{0, 0.1, 0.2\}$ are strongly unstable and develop a bar, all on about the same time-scale. The models with $r_a=\{0.3, 0.5\}$ appear to be stable, or very nearly so. The uncertainty is due mostly to numerical effects associated with the particle softening. In the runs with large softening the

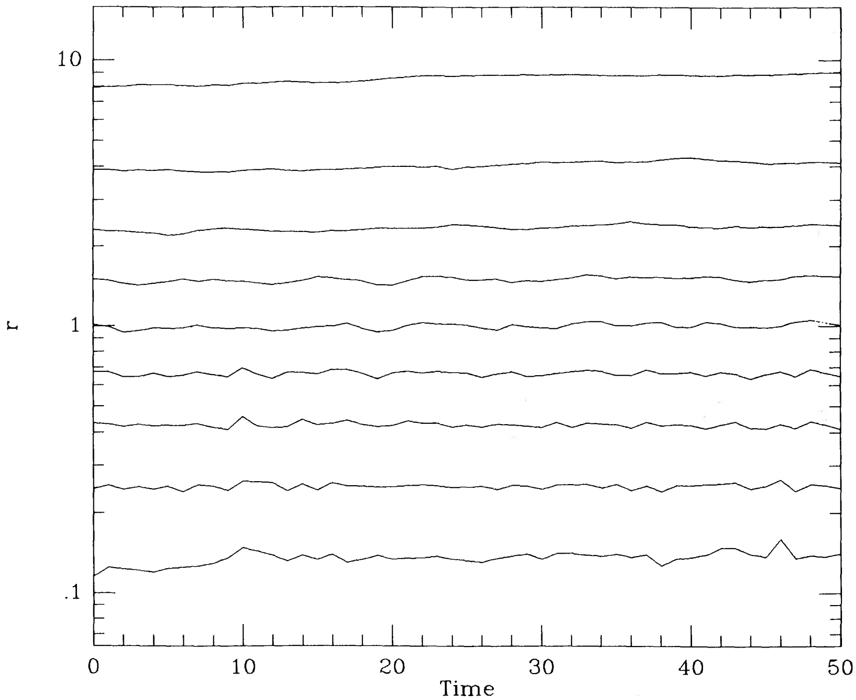

Figure 4. Evolution of the radii containing 10, 20, . . . 90 per cent of the mass for the run shown in Fig. 1.

potential is poorly represented near the centre; as a result, the radii containing 10 and 20 per cent of the mass expand by ~ 30 per cent initially, and the velocities become temporarily more radial. This initial readjustment is probably responsible for the apparent instability of the $r_a=0.3$ model when $\varepsilon=0.03$. The same model shows only a hint of growing ellipticity when the softening length is reduced. We conclude that the $r_a=0.3$ model is probably stable, but lies close to the stability boundary.

(ii) *The instability produces no discernible change in the radial distribution of matter.* Fig. 4 shows the evolution of the radii containing 10 per cent, 20 per cent, etc. of the mass for the run of Fig. 1. There is a slight initial readjustment due to the finite softening length, and a slow overall expansion due to the non-conservation of energy, but no significant change associated with the formation of the bar at $t\approx 10$.

(iii) *The instability tends to produce nearly prolate bars with a characteristic axis ratio between 2 and 2.5, regardless of the degree of anisotropy of the initial model.* Fig. 5 shows the final ratio of long to short axes as a function of fractional mass for each of the runs. At mass levels corresponding to $r\gtrsim 3r_a$, all the unstable models have about the same final elongation, and there is only a slight dependence of elongation on radius. Once again the results depend somewhat on the softening length. When the softening is large, the bars maintain a nearly constant elongation after they form; but for smaller softenings there is a gradual evolution (quite marked when $\varepsilon=0.003$) toward sphericity, especially at small radii. We feel certain that this gradual evolution is a result of momentum exchange beween individual particles, which should be significant in the runs with the smallest softenings. The complex way that our computer code computes the force associated with each particle (*cf.* McGlynn 1984) makes it difficult to predict the time-scale for these spurious relaxation effects, but the fact that they depend strongly on the softening length reassures us that they would be of negligible importance in a real galaxy.

Only the purely radial model develops a significant triaxiality, with an intermediate-to-short axis ratio $Y/Z\approx 1.4$ at the final time-step. The other models remain about as axisymmetric as the isotropic (stable) model, i.e. $Y/Z\lesssim 1.1$

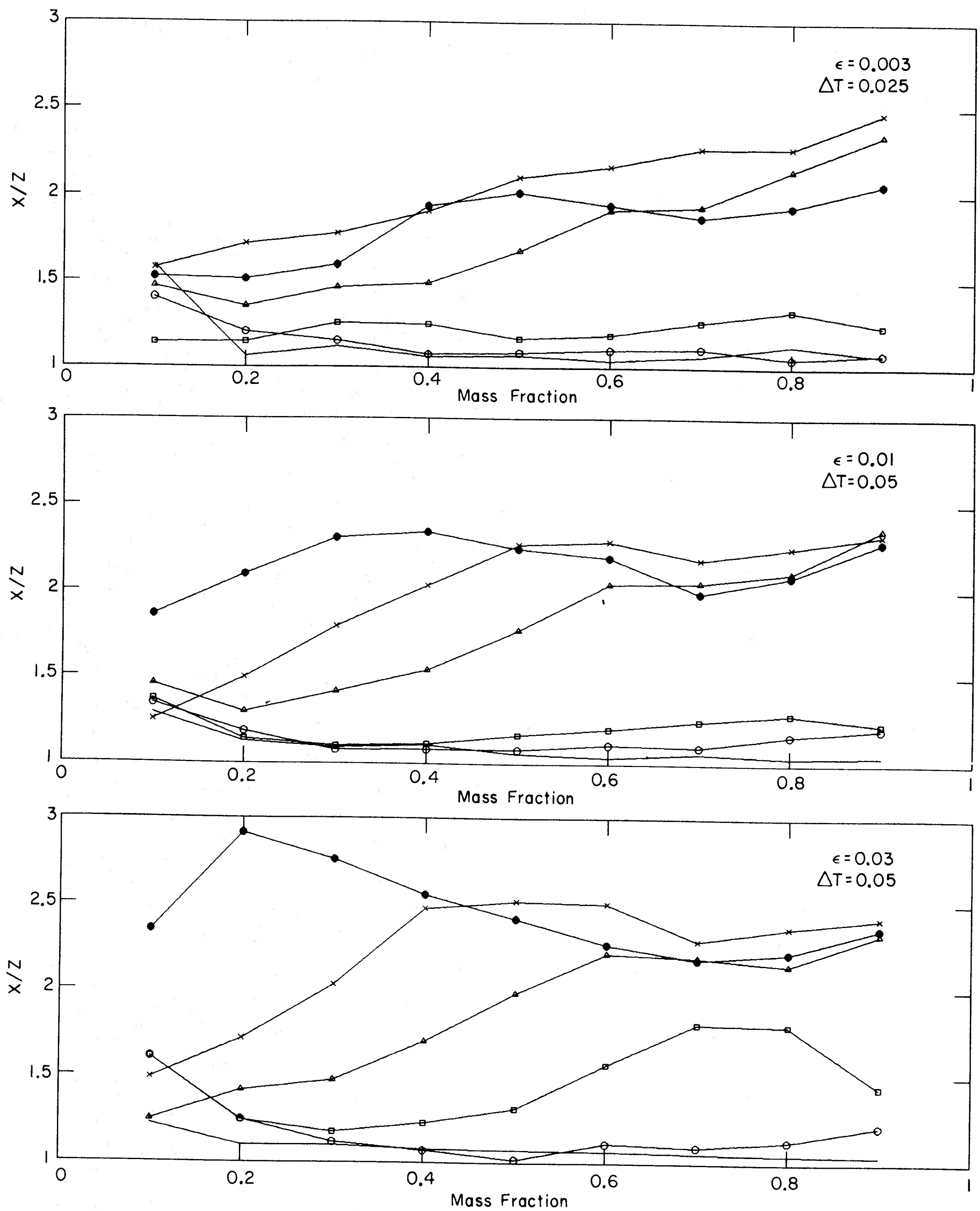

Figure 5. Final axis ratios as a function of mass for the runs from Family 1. Symbols are defined in Table 1.

3.3 STABILITY BOUNDARY

The very marked difference in behaviour of models with r_a=0.2 and r_a=0.3 suggests that the stability boundary lies somewhere between these two models, i.e. at a global anisotropy of $2T_r/T_t \approx 2.5$. The uncertainty associated with this number is difficult to estimate. Even the r_a=0.5 model shows a hint of growing ellipticity compared to the (stable) isotropic model, and might conceivably be judged unstable on a very long time-scale. What we can say with some certainty is that the stability properties of these models change dramatically as r_a is decreased from 0.3 to 0.2.

This conclusion is reasonably unaffected by uncertainties associated with the softening length, since the very small softenings used in some of the runs allow the initial state of models near the stability boundary to be represented quite accurately, and the accumulated errors due to shell crossings should not be too important in the time it takes the instability to develop.

4 Stability of two additional families

The N-body calculations just described demonstrate the importance of the radial-orbit instability in galaxy models with realistic density profiles. Another important question is the universality of the instability: i.e. will *any* spherical model with a sufficient amount of radial motion be unstable, or does the stability 'boundary' depend strongly on details of the orbital distribution? The results obtained so far provide at least part of the answer: the global anisotropy parameter $2T_r/T_t$ is *not* a good indicator of instability. In the generalized polytropic models analysed by Fridman & Polyachenko (1984) and Barnes, Goodman & Hut (1985), instability appeared to be present whenever $2T_r/T_t \geqslant 1.4$. In the models analysed here the critical value appears to lie between 2.3 and 2.9. Now the polytropic models differ from those analysed here in two important respects: their mass is less centrally concentrated, and their velocity ellipsoids have a fixed elongation (as opposed to spherical at the centre and elongated at large radii). The possible importance of the density profile in determining stability will not be considered here; observed elliptical galaxies are so uniform in their luminosity distributions that little of astrophysical importance would be learned by varying the density profile.

On the other hand, it seems intuitively obvious that the radial variation of the velocity ellipsoid could have a *strong* effect on the stability. Consider a model in which the core is populated by eccentric orbits, while the outer, massive halo is nearly isotropic. (Just such a model has been proposed for the giant galaxy M87; *cf.* Binney & Mamon 1982). The *global* anisotropy of such a model would always be close to unity, but the central regions would be dynamically uncoupled from the halo and almost certainly unstable. The same argument does not apply to models (such as the ones analysed above) that are isotropic in the centre and radial farther out, since the eccentric orbits responsible for the instability must pass through the isotropic, and presumably stabilizing, core. Indeed, all of the models analysed above are almost completely radial outside the half-mass radius, but only some are unstable. It seems likely, therefore, that stability is strongly dependent on the behaviour of the velocity ellipsoid near the centre.

These arguments led us to consider the stability properties of two additional families of models with the same density law (1), but different dependences of velocity anisotropy on radius. Family 2 was defined simply as the linear superposition of the radial orbit ($r_a=0$) and isotropic ($r_a\rightarrow\infty$) models defined above. The global anisotropy of these models may be written in terms of the fraction of mass in radial orbits α as $2T_r/T_t=(2\alpha+1)/(1-\alpha)$; the local anisotropy turns out to be greatest at the centre and to decline with radius. Family 3 was generated from a distribution function of the form.

$$f(E,\ J^2)=J^{2m}g(E), \qquad -1\leq m\leq\infty,$$

which yields a model with *constant* anisotropy $2T_r/T_t=(m+1)^{-1}$. An algorithm for deriving $g(E)$ from $\varrho(r)$ is given by Merritt (1985c, in preparation). The initial parameters of these models are given in Table 1.

Fig. 6 shows the evolution of a set of models from Family 2 with global anisotropies equal to those of the six models tested above, as well as two models with $2T_r/T_t=1.4$ and 1.2. All runs were made with $\varepsilon=0.01$. The differences between the stability properties of this family and the previous one are striking: instead of a sudden transition to instability, these models appear to become *gradually* more unstable as the orbital distribution is made more radial, and their final

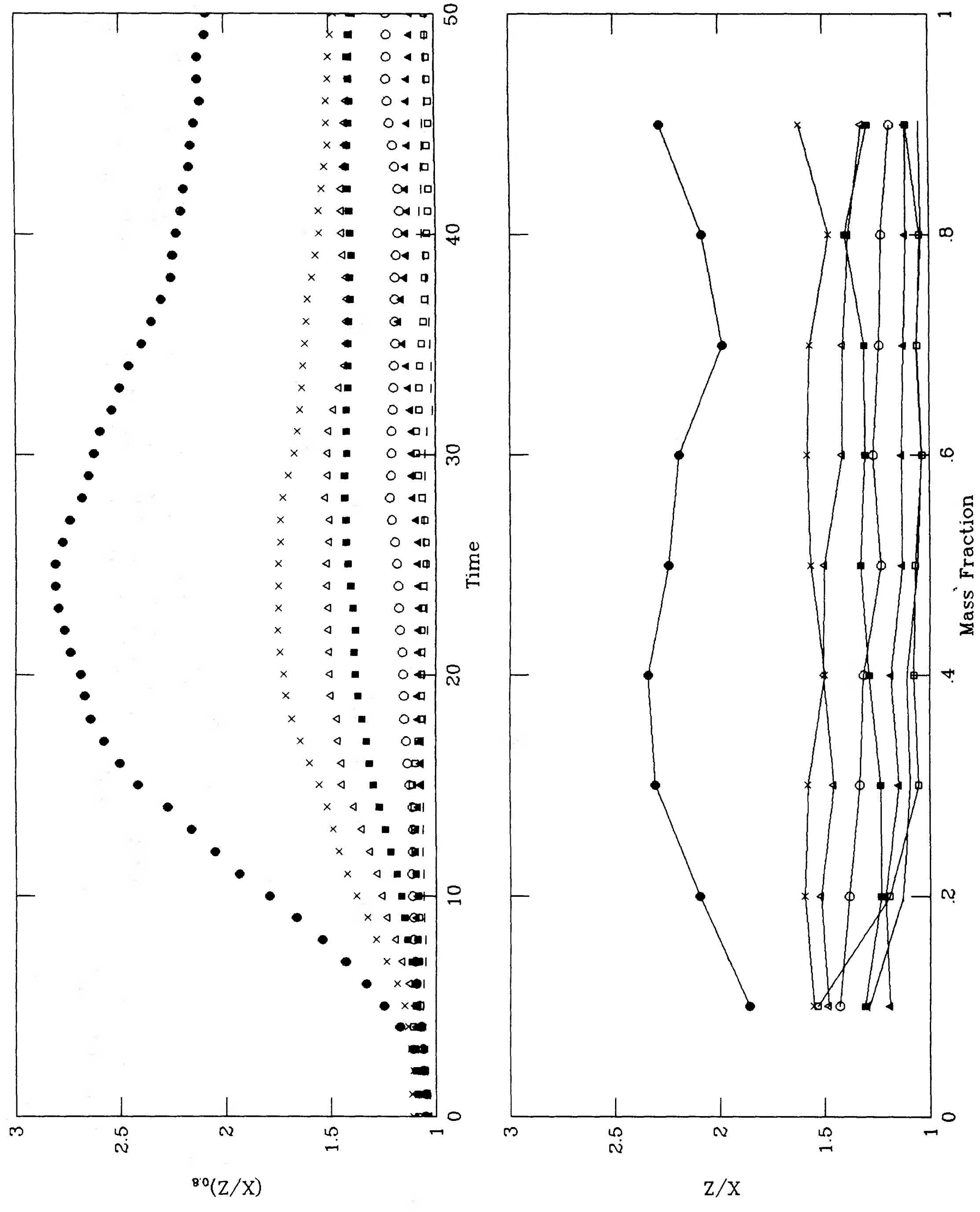

Figure 6. Evolution of the axis ratios of the most bound 80 per cent of the mass, and final axis ratios as a function of mass, for the runs from Family 2. Symbols are defined in Table 1.

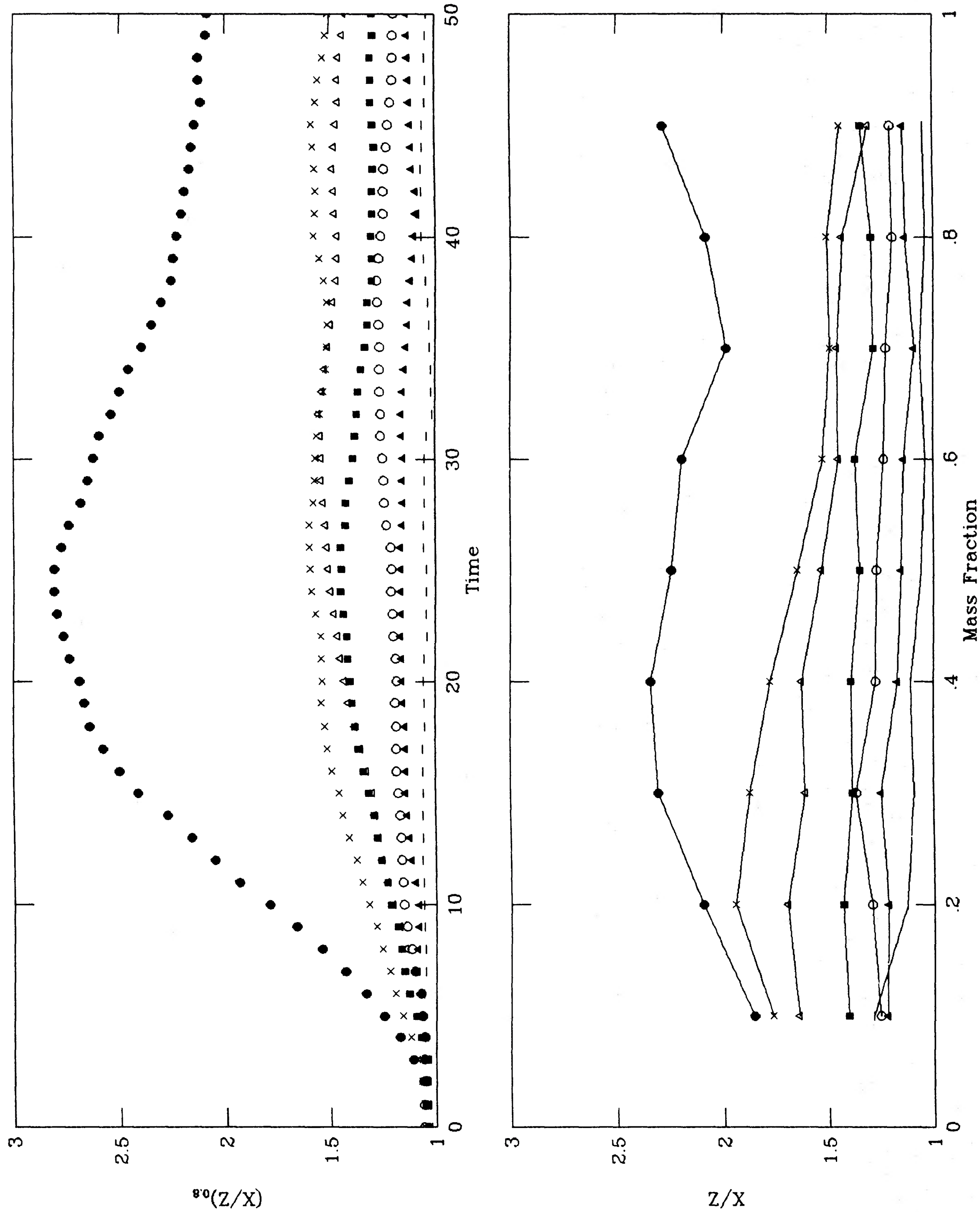

Figure 7. Same as Fig. 6, but for Family 3. Symbols are defined in Table 1.

elongation depends strongly on their initial anisotropy. Only the $2T_r/T_t=1.2$ model appears to be 'as stable' as the isotropic model. The models from Family 3 behave in a very similar way (Fig. 7).

This behaviour is very similar to that found by BGH for a family of 'polytropic' models with anisotropy independent of radius. They found, as we do here, that even models as isotropic as $2T_r/T_t=1.4$ evolve significantly more than isotropic models. On the other hand, it is not clear whether the small amounts of 'evolution' seen by us and BGH in the models with small anisotropy are indicative of instability, or of spurious evolution due to the approximate way in which the computer code computes the potential. It is significant that both models from Family 2 with $2T_r/T_t<1.8$ show even *less* evolution than the two models form Family 1 with $r_a=\{0.3, 0.5\}$ judged 'stable' above. Because of this we are very uncertain where to place the stability boundary for Families 2 and 3. Subsequent work should probably be directed toward understanding the systematic errors associated with N-body codes of the type used here and by BGH.

What we *can* say is that the instability manifests itself very differently in these three families of models, and that Families 2 and 3 are still unstable at values of the global anisotropy for which Family 1 appears to have already crossed the boundary from instability to stability. Taken together with the results of BGH, our results reinforce the conclusion that the stability of a given equilibrium configuration depends on the radial variation of the velocity ellipsoid, as well as the total amount of radial motion, among other possible factors. In particular, models with isotropic cores appear to be 'more stable', in the sense just defined, than models dominated by radial orbits near the centre.

The models of Family 3 are particularly interesting because (with the exception of the $m=-1$ model) they satisfy the inequalities $\{\partial f/\partial E<0, \partial f/\partial J^2<0\}$ for all (E, J). According to a proof of Gillon, Doremus & Baumann (1976), models satisfying these conditions should be stable. Unless the numerical simulations described here are somehow misleading, we are forced to conclude that their stability proof is incorrect. Our results do not contradict a number of other proofs (e.g. Doremus & Feix 1973) concerning the stability of anisotropic systems to purely radial perturbations.

5 Implications of the radial orbit instability for dynamical studies of elliptical galaxies

An interesting question raised by these calculations is whether past work on the dynamics of elliptical galaxies, which are often idealized as anisotropic spherical systems, is self-consistent. Unfortunately this question cannot be answered in a very definite way. Following Binney (1980), the dynamics of spherical galaxies have usually been discussed from a 'local' or 'hydrodynamic' point of view, in which the radial dependence of the velocity anisotropy is specified without regard to the existence of an equilibrium distribution function (e.g. Binney & Mamon 1982; Tonry 1983). Only recently have attempts been made to derive proper distribution functions from density and velocity measurements (e.g. Richstone & Tremaine 1984; Newton & Binney 1984; Merritt 1985a), but so far these techniques have not been applied to a large number of galaxies. Incumbent on future studies will be the necessity of demonstrating that a proposed spherical model is stable. Our results suggest that models dominated by eccentric orbits near the centre are especially likely to be unstable. Such models have been widely discussed in connection with the giant elliptical galaxy M87 (e.g. Binney & Mamon 1982).

Presumably the same caution should be applied to triaxial models, although little is known yet about the equilibrium states of systems with three integrals of motion.

6 Stability of radial collapse

If spherical models for elliptical galaxies are often unstable to the formation of a bar, it is natural to wonder at what point during the formation of such a galaxy the instability would take an active role in determining its shape. That this is a promising line of inquiry is suggested by the results of van Albada (1982) and McGlynn (1984), who find that dissipationless collapse can produce galaxies with realistic density profiles only if the initial state is very cold. Collapse from a cold, spherical cloud will produce a final system that is dominated by radial orbits, and therefore potentially unstable. The radial orbit instability could therefore be an important determinant of the final shapes of galaxies that formed via dissipationless collapse.

We can use the results of Section 3 to estimate how cold an initially spherical cloud must be if the galaxy into which it forms will be unstable. Spherical collapse has the property of exactly conserving the angular momentum of each particle, regardless of its change in energy. Now the total squared angular momentum per unit mass (defined as the sum of the squares of the angular momentum of each particle) of the models from Family 1 is roughly equal to $J^2 \approx 2r_a^2T_t/M \approx GMr_a^2/2r_0(1+T_r/T_t)$; the latter expression follows from the virial theorem, and the fact that the total potential energy is equal to $-GM^2/2r_0$ for a model with the density law (1). Suppose that such a galaxy formed from the dissipationless collapse of a cloud with no systematic velocities. This assumption is reasonable because the models from Family 1 are quite similar to those formed in collapse simulations, both in terms of their density and velocity structure (Merritt 1985a; van Albada 1982). Assume an initial density profile for the cloud of $\varrho \propto r^{-1}$, and a Maxwellian distribution of particle velocities. (These are the initial conditions adopted below.) The internal angular momentum of such a cloud is easily shown to be $J^2=(2\pi/81)GMR_1(2T/W)$, where R_1 is its outer radius and T/W is the ratio of kinetic to potential energies, i.e. $T/W=3\sigma^2R_1/2GM$. Equating the two angular momenta, and requiring the energies of the initial and final states to be the same (ie. $r_0=3R_1/4$), yields the following relation between initial temperature and final anisotropy:

$$\frac{2T}{W} \approx 5\left(\frac{r_a}{r_0}\right)^2\left(1+\frac{T_r}{T_t}\right)^{-1}. \tag{3}$$

Since the equilibrium models are unstable for $r_a \lesssim 0.3r_0$ and $2T_r/T_t \gtrsim 2.3$, the critical initial temperature is $2T/W \approx 0.2$. Collapse from colder initial conditions would be expected to lead to an elongated final state.

To test this hypothesis, we computed the collapse and relaxation of a set of spherical clouds with low initial temperatures. To avoid having to deal with near-infinite densities at the point of maximum collapse, the particles were initially laid down with an r^{-1} density profile. The initial distribution of velocities was assumed to be Maxwellian and independent of radius; the cut-off radius R_1 was chosen so as to make the initial energy equal to that of the equilibrium models considered above. Evolution was computed using 5000 particles, a softening length of 0.5 and a time-step of 0.05; energy was conserved to <5 per cent, most of the error occurring around the time of maximum collapse.

Fig. 8 illustrates the collapse of a sphere with initial temperature $2T/W=0.02$. Because the density is initially a decreasing function of radius, the collapse time is shortest at the centre. Elongation is first apparent at $T \approx 5$, after a substantial fraction of the mass has fallen in and begun to re-expand. The most bound 80 per cent of the mass attains an equilibrium elongation of $X/Z \approx 2.3$; the global anisotropy $2T_r/T_t$ decreases from ~ 25 at $T=2$ to ~ 5 at $T=5$ and ~ 3 at $T=10$. As expected, initially spherical collapse can lead to a highly elongated final state.

Fig. 9 shows the dependence of the final elongation on the initial temperature for a set of seven collapses. As predicted, collapses starting from initial conditions with temperatures $2T/W \lesssim 0.2$ lead to a bar. The characteristic axis ratio is $2 \lesssim X/Z \lesssim 2.5$, and the elongation is nearly independent of radius, just as in the bars formed from the unstable equilibrium models of Family 1.

It is curious that earlier workers did not notice the instability of radial collapse to bar formation. The primary reason is undoubtedly that few simulations have been performed starting from

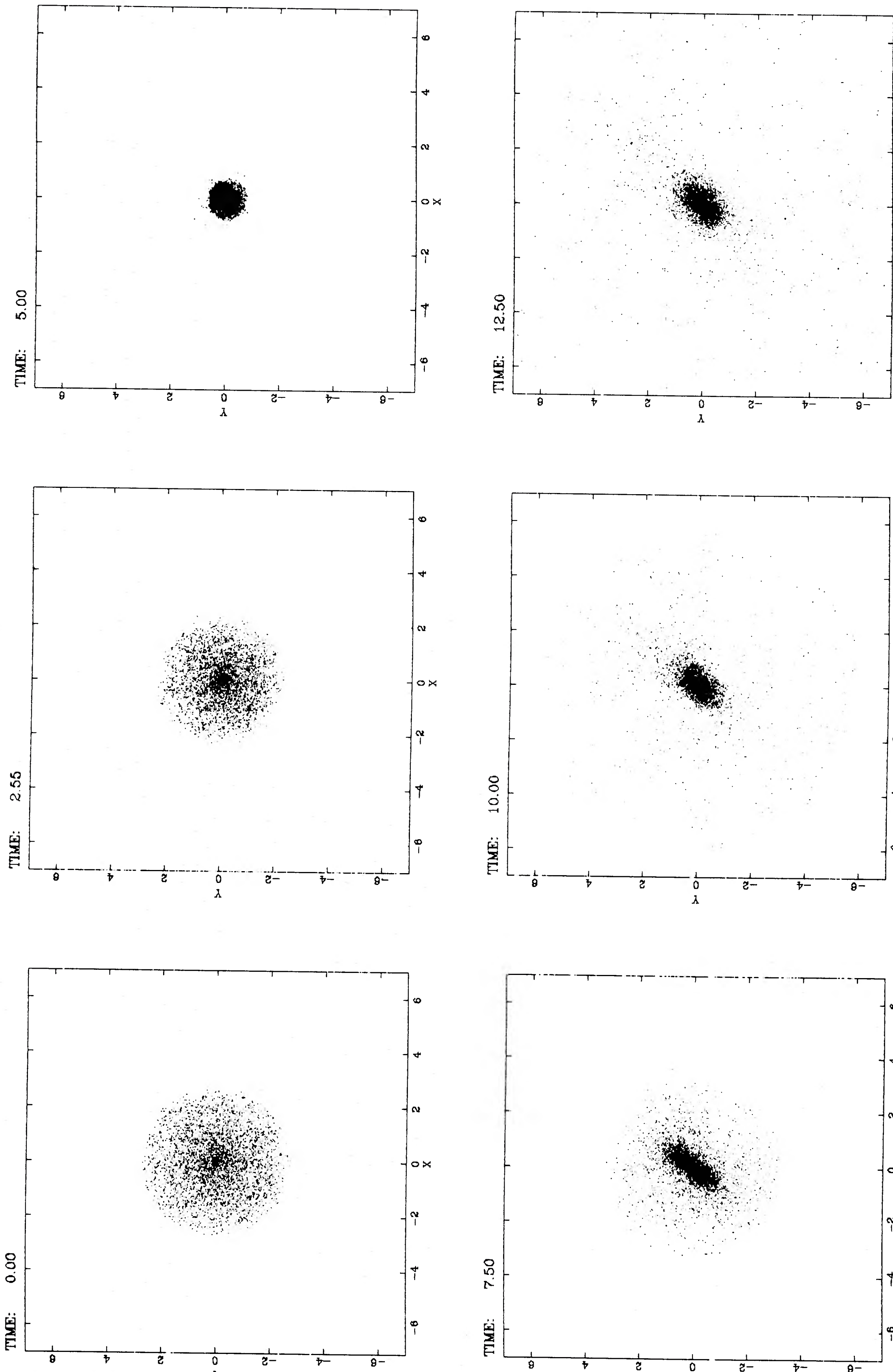

Figure 8. Snapshots at six time-steps of the collapse starting from a cloud with temperature $2T/W=0.02$. The view is from a direction such that the principal axes at the final time-step lie in the plane of the paper.

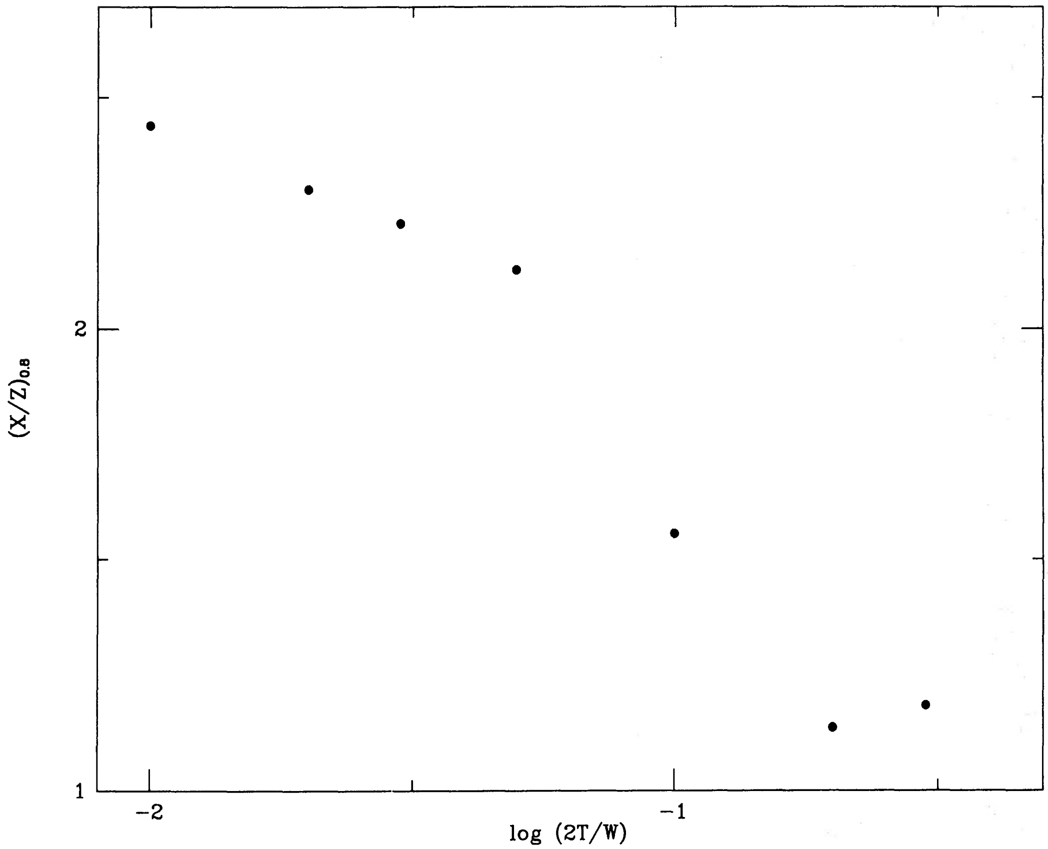

Figure 9. Dependence of the final elongation on the initial temperature for the collapse simulations.

sufficiently cold initial conditions; for instance van Albada (1982) considers no collapses with $2T/W<0.1$. Other workers have *imposed* spherical symmetry throughout the collapse (e.g. Fujiwara 1983; Pryor & Lecar 1983). On the other hand, Peebles (1970) calculated completely self-consistent collapses of 300 particle systems starting from completely cold initial conditions. He does not discuss the shapes of his final models however. We suspect that the radial orbit instability was active in many of the collapse simulations described in the literature, and went unnoticed only because of a preconception that spherical initial conditions should lead to a spherical final state.

One way in which the instability manifests itself differently in the collapse simulations than in the initially equilibrium models is in its effect on the radial distribution of matter. Collapses in which the instability plays a significant role produce less centrally concentrated final states than would be expected in the absence of the instability. Fig. 10 shows the final central concentration (defined as the ratio of the radii containing 50 and 10 per cent of the mass) of each of the collapse simulations, as well as the central concentrations of a set of runs evolved with a 'monopole' code, i.e. a code in which the potential is computed by an unweighted angular average of the particle positions. Collapses computed with the monopole code are guaranteed to remain spherically symmetric. Fig. 10 shows that unstable collapses produce a characteristic central concentration of $r_{0.5}/r_{0.1}\approx 4$, while in purely radial collapses the central concentration increases monotonically as the initial temperature is reduced. We conclude that the radial orbit instability can play a significant role in 'decoupling' final and initial states during dissipationless collapse.

What relation, if any, do these collapse simulations have to the problem of galaxy formation? Phase-space density constraints (Tremaine 1985) may be used to show that an intially uniform

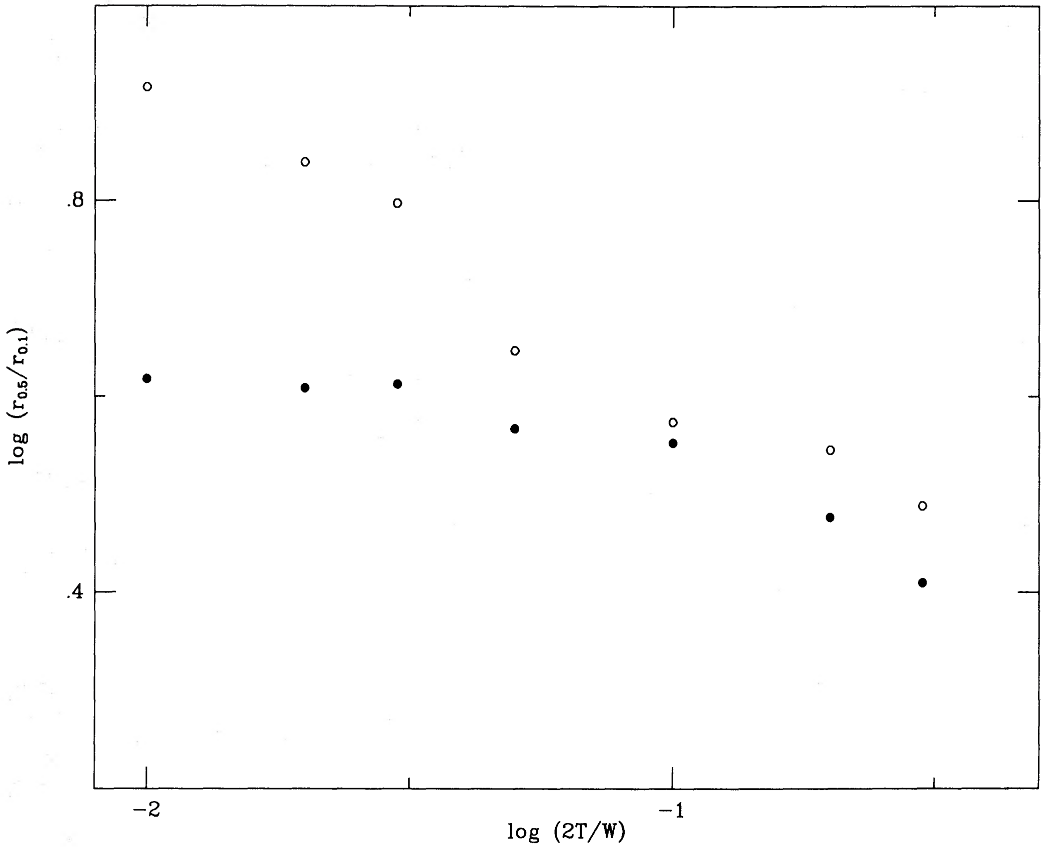

Figure 10. Central concentrations (defined in the text) of the collapse simulations at the final time-step. Filled circles: quadrupolar code. Open circles: spherically symmetric code.

cloud must be very cold, $2T/W \lesssim 0.02$, if the galaxy into which it forms is to be as centrally condensed as real elliptical galaxies. However, these constraints can also be satisified by an intially hotter, clumpy medium (Tremaine 1985), and in fact clumpy initial conditions seem to be very effective at producing galaxies with the right density profiles (van Albada 1982). Furthermore, the currently most popular theories for the origin of galaxies all predict that galaxies would form from the amalgamation of smaller lumps, and not from a uniform cloud (e.g. Efstathiou & Silk 1983). Finally, most protogalactic density fluctuations would presumably be non-spherical, and it is well known that flattening tends to increase during collapse, even in the absence of instabilities like the one discussed here (Lin, Mestel & Shu 1965). The case for very cold, uniform and spherical initial conditions is therefore not very strong.

On the other hand, we can see no reason why the radial orbit instability should not play a role, albeit a modified one, in more realistic collapses. If this hypothesis can be shown to be true, it might greatly alter our ideas about violent relaxation, and provide an important clue toward understanding the uniformity of elliptical galaxies.

Acknowledgments

The authors thank S. White for advice on using the N-body code, and S. Tremaine for suggesting that we check the stability of models with $\partial f/\partial E<0$. This work was supported in part by NSF grant AST 81-18557, and by a Grant-in-Aid of Research from the Sigma Xi Society. We are grateful to the astronomy department at U. C. Berkeley for generous allocation of computer time.

References

Aarseth, S. J., 1967. *Bull. Astronomique,* **3,** 47.
Aguilar, L. A. & White, S. D. M., 1985. *Astrophys. J.,* **295,** 374.
Antonov, V. A., 1960. *Astr. Zh.,* **37,** 918 (translated in *Soviet Astr.,* **4,** 859).
Antonov, V. A.., 1962. Vestnik Leningrad Univ., **19,** 96 (translated in Princeton Plasma Pys. Lab. Rept. PPL-Trans-1).
Barnes, J., Goodman, J. & Hut, P., 1985. Preprint.
Binney, J., 1980. *Mon. Not. R. astr. Soc.,* **90,** 873.
Binney, J. & Mamon, G. A., 1982. *Mon. Not. R. astr. Soc.,* **200,** 36.
Doremus, J. P. & Feix, M. R., 1973. *Astr. Astrophys.,* **29,** 401.
Efstathiou, G. & Silk, J., 1983. *Fund. Cosmic Phys.,* **9,** 1.
Fridman, A. M. & Polyachenko, V. L., 1984. *Physics of Gravitating Systems,* Vol. 1 and Vol. 2, Springer.
Fujiwara, T., 1983. *Publs Astr. Soc. Japan, 35,* 547.
Gillon, D., Doremus, J. P. & Baumann, G., 1976. *Astr. Astrophys.,* **48,** 467.
Henon, M., 1973. *Astr. Astrophys.,* **24,** 229.
Jaffe, W., 1983. *Mon. Not. R. astr. Soc.,* **202,** 995.
Lin, C. C., Mestel, L. & Shu, F. H., 1965. *Astrophys. J.,* **142,** 1431.
McGlynn, T. A., 1984. *Astrophys. J.,* **281,** 13.
Merritt, D., 1985a. *Astr. J.,* **90,** 1027.
Merritt, D., 1985b. *Mon. Not. R. astr. Soc.,* **214,** 25P.
Newton, A. J. & Binney, J., 1984. *Mon. Not. R. astr. Soc.,* **210,** 711.
Peebles, P. J. E., 1970. *Astr. J.,* **75,** 3.
Polyachenko, V. L., 1981. *Pis'ma Astr. Zh.,* **7,** 142 (translated in *Soviet Astr. Lett.,* **7,** 79).
Polyachenko, V. L. & Shukhman, I. G., 1981. *Astr. Zh.,* **58,** 933 (translated in *Soviet Astr.,* **25,** 533).
Pryor, C. & Lecar, M., 1983. *Astrophys. J.,* **269,** 513.
Richstone, D. O. & Tremaine, S., 1984. *Astrophys. J.,* **286,** 27.
Tonry, J. L., 1983. *Astrophys. J.,* **266,** 58.
Tremaine, S., 1985. Preprint.
van Albada, T. S., 1982. *Mon. Not. R. astr. Soc.,* **201,** 939.